EUROPHYSICS LETTERS 1 August 2002

Europhys. Lett., **59** (3), pp. 384–390 (2002)

Influence of self-assembly on dynamical and viscoelastic properties of telechelic polymer solutions

D. Bedrov[1], G. D. Smith[1] and J. F. Douglas[2]

[1] *Department of Materials Science & Engineering, University of Utah*
122 S. Central Campus Drive, Room 304, Salt Lake City, UT 84112, USA
[2] *Polymers Division, National Institute of Standards and Technology*
Gaithersburg, MD 20899, USA

(received 4 February 2002; accepted in final form 30 April 2002)

PACS. 61.25.Hq – Macromolecular and polymer solutions; polymer melts; swelling.
PACS. 62.10.+s – Mechanical properties of liquids.
PACS. 62.25.+g – Mechanical properties of nanoscale materials.

Abstract. – Incipient micellization in a model self-associating telechelic polymer solution results in a network with a transient elastic response that decays by a two-step relaxation: the first is due to a heterogeneous jump-diffusion process involving entrapment of end-groups within well-defined clusters and this is followed by rapid diffusion to neighboring clusters and a decay (terminal relaxation) due to cluster disintegration. The viscoelastic response of the solution manifests characteristics of both a glass transition and an entangled polymer network.

The formation of clusters that associate and dissociate in dynamic equilibrium is a ubiquitous natural phenomenon comparable to phase separation and liquid condensation in its scope and ramifications. Dynamical clustering occurs in micelle formation, equilibrium polymerization, nanoparticle solutions, thermally reversible gelation and a variety of biological self-organization processes [1]. While there has been much effort to describe thermodynamic aspects of particle clustering transitions, there is limited understanding of the changes in dynamical solution properties that accompany these transitions and how these changes relate to the molecular motions of associating particle systems. Dudowicz *et al.* has emphasized the common nature of the thermodynamic properties of these transitions [1], and some commonality in the dynamical properties might be expected.

Molecular simulations have made important contributions to our understanding of polymer self-association. Molecular dynamics (MD) and Monte Carlo (MC) simulation studies of telechelic (chains with attractive end-groups) polymer solutions [2–4], as well as micelle-forming monochelic surfactant solutions (*e.g.*, [5, 6]), have been reported in the literature. These studies focused on the extent of micellization and factors that influence micelle size and shape distribution. Groot and Agterof [7] used a MC off-lattice simulation model to study viscoelastic properties of associative polymer networks and found interesting parallels between their idealized model and entangled polymer solutions. More recently, Kumar and Douglas [8] utilized lattice MC simulations to study the dynamic properties of self-associating

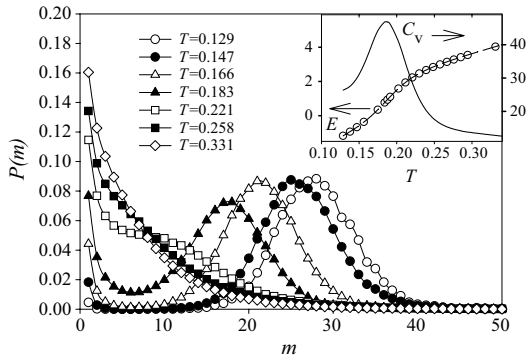

Fig. 1 – The probability of finding an end-group in a cluster of size m for the telechelic polymer solution over a wide range of temperatures. The inset plot shows the temperature dependence of the total energy and isochoric heat capacity in the system as a function of temperature. Uncertainties are smaller than the size of the symbols.

polymers with regularly spaced stickers. They observed the onset of thermoreversible gelation, corresponding to a sticker clustering transition and noted a similarity of the dynamics of these systems with incipient glass formation in molecular liquids. In spite of these important studies, molecular simulations have yet to provide a clear mechanistic understanding of the dramatic changes in dynamic and viscoelastic response of self-associating polymers that occur as a consequence of dynamic clustering for even simple model systems. Since there are always questions about the faithfulness of MC simulation to the dynamics of real fluids, we further investigate this type of problem through MD simulation of a minimal model of an associating (micelle forming) liquid to determine if dynamical features similar to those found previously are recovered and to come to a more fundamental molecular understanding of the dramatic changes in dynamic and viscoelastic response of self-associating polymers that occur as a consequence of dynamic clustering. Specifically, we performed MD simulations on an ensemble of bead-necklace telechelic polymers consisting of eight beads. All beads experienced excluded-volume interactions modeled by a shifted and truncated Lennard-Jones potential [9] with an (unshifted) Lennard-Jones well depth (ε) of 1/9 and the bead diameter σ defines the unit of length. An additional attractive end-group/end-group interaction of unit magnitude [2–4] (truncated at 2.5) was employed. MD simulations were performed on an ensemble of 1000 chains at $\rho = 0.2$ [10] in an NVT ensemble using the simulation package *Lucretius* [11]. All properties reported below are expressed in terms of the energy and length scales, ε and σ, respectively [12]. Uncertainties were estimated using 68% confidence standard error analysis [13] for several statistically independent subsets of the trajectories.

First, we briefly characterize equilibrium aspects of micelle formation in this model telechelic solution. Figure 1 shows the probability $P(m)$ of finding an end-group in a cluster of size m, while the inset plot shows the total energy (E) and heat capacity (C_v) of the solution as a function of temperature (T). At all T investigated, we found extensive clustering as well as geometric percolation as a consequence of polymer chains spanning the space between clusters. (See [8] for similar phenomena in the case of thermally reversible gelation.) For $T > 0.221$, $P(m)$ decreases monotonically with increasing cluster size and the clusters are relatively small and spatially diffuse. Near $T = 0.221$ we observe the emergence of a shoulder in $P(m)$, which we take as the onset of micelle formation (T_x). At lower T this shoulder transforms into a pronounced peak. Compact clusters that increase in size (number of end-groups), but not in

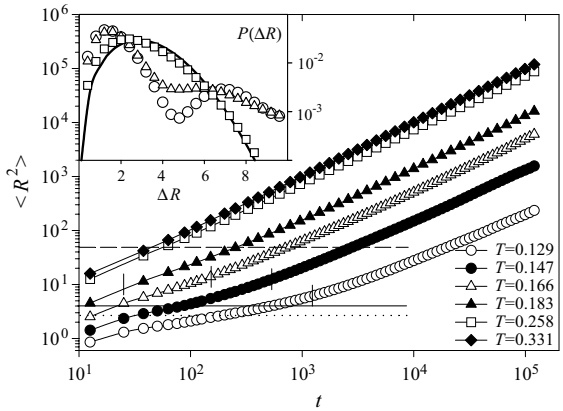

Fig. 2 – End-group $\langle R^2 \rangle$ as a function of time at various temperatures. Horizontal lines indicate the mean cluster size (which is roughly independent of T) determined from the mean end-group cluster R_{g} (dotted line) and end-group displacement distribution (solid line). The dashed horizontal line indicates the length scale associated with end-group hops. Vertical lines correspond to the maximum in non-Gaussianity associated with the end-group caging time. Inset plot shows the distribution of end-groups displacements over time intervals corresponding to $\langle R^2 \rangle \approx 12$ (maximum in non-Gaussianity parameter) for various T (the temperature-symbol correspondence is the same as on the main plot) as well as the Gaussian distribution with the same $\langle R^2 \rangle$ (solid line). Estimated uncertainties are smaller than the size of the symbols.

spatial extent (defined as radius of gyration of the cluster) with decreasing temperature are manifested when $T < T_x$. After the onset of micellization we do not observe additional qualitative changes in $P(m)$ with further reduction in temperature. The suggested micellization mechanism is further supported by strong changes in E for $T < T_x$ and a maximum in C_v. The T at which C_v has a peak ($T \approx 0.18$) is identified with thermodynamic micelle transition temperature T_{m} so that $T_x/T_{\mathrm{m}} \approx 1.2$.

Next, we consider the changes in dynamical and viscoelastic properties that accompany micellization. In fig. 2 we show the mean-square displacement ($\langle R^2 \rangle$) of end-groups. For $T < 0.221$, the $\langle R^2 \rangle$ exhibits an inflection point that for lower temperatures evolves into three clearly identifiable displacement regimes: ballistic motion at short times, displacement localization ("caging") at intermediate times, and diffusive transport at long times. At higher T caging effects are not observed in the end-group motion. The onset of end-group caging correlates well with the onset of micellization discussed above. Specifically, the formation of well-defined clusters at lower T results in caging of the end-groups within the dimensions (R_{g}) of the cluster, followed by "hopping" of the end-group to another cluster at longer times. Since the hopping process is rapid compared to the mean residence time of an end-group within a cluster (caging time), end-group dynamics on the caging time scale are relatively heterogeneous. On shorter and longer time scales the end-group dynamics are more homogeneous: either all end-groups are restricted to motion within the cluster (caged motion, short times) or all end-groups have hopped many times (diffusive motion, long times). This dynamic heterogeneity is reflected in a strongly non-Gaussian character of the end-group displacement distribution, quantified by the second cumulant of the distribution, at the time scale of caging. The maximum in the non-Gaussianity establishes the caging time scale for each temperature [14], which is shown in fig. 2. For $T < T_x$, the caging time scale corresponds to a $\langle R^2 \rangle$ of around 10. On this scale the distribution of end-group displacements is highly

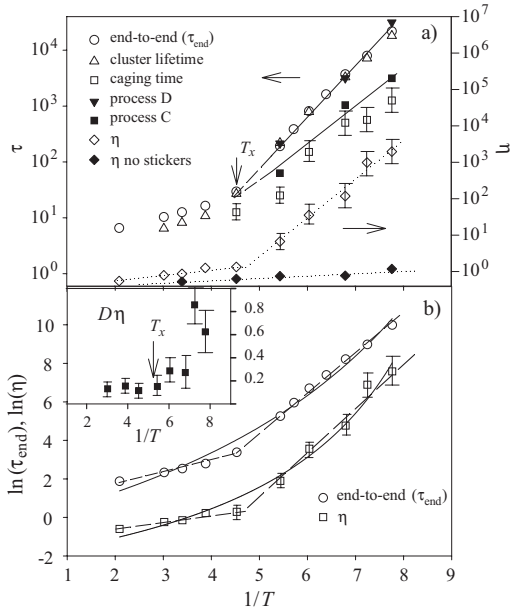

Fig. 3

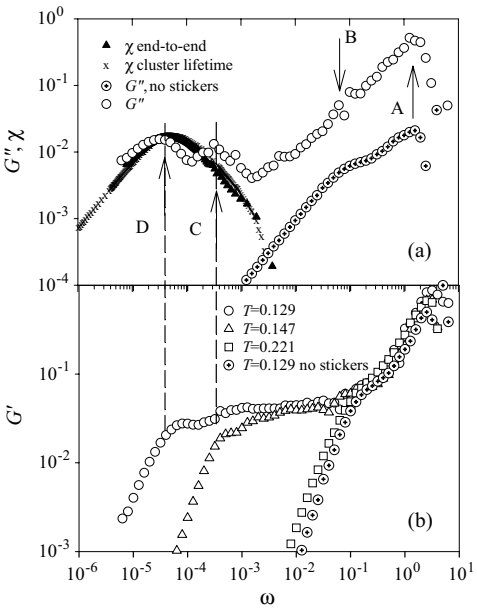

Fig. 4

Fig. 3 – a) End-to-end vector $V(t)$ and cluster lifetime $C(t)$ relaxation times, caging time, processes (D) and (C) and viscosity for the telechelic solutions as a function of inverse temperature; b) Vogel-Fulcher (solid line) and Arrhenius (dashed line) fits of $\tau_{\rm end}$ and η as a function of T. The inset plot shows the product of self-diffusion coefficient and viscosity *vs.* $1/T$. Estimated uncertainties are either smaller than the symbol size or shown explicitly using error bars.

Fig. 4 – a) The mechanical, end-to-end and cluster lifetime dynamic susceptibilities as a function of angular frequency for the telechelic solution and the solution without end-group attraction for $T = 0.129$. b) The shear storage modulus as a function of angular frequency for the telechelic solution and the solution without end-group attraction at various T.

non-Gaussian with clear peaks at distances corresponding to the $R_{\rm g}$ of the cluster ($R_{\rm g} \approx 2$) and the mean distance between clusters (≈ 7) as shown in fig. 2 (inset). These length scales correspond to the caging length scale and the onset of diffusive motion, as shown in fig. 2. For $T > T_x$, the displacement distribution is featureless and nearly Gaussian on this length scale. This caging phenomenon is similar to recent lattice MC simulations of thermoreversible gelation in associating polymer solutions, having many sticker groups along the chain [8]. Kumar and Douglas [8] have emphasized the similarity of this caging phenomenon in the particle displacements to simulations of the dynamics of incipient glass-formation [14]. The present paper goes beyond this previous study by systematically examining corresponding changes in viscoelastic properties of a model associating fluid.

We also investigated the chain end-to-end vector autocorrelation function $V(t)$ and cluster lifetime autocorrelation function $C(t)$. The latter is given as

$$C(t) = \frac{\sum_{i \neq j} H_{ij}(t) \cdot H_{ij}(0)}{\sum_{i \neq j} H_{ij}(0) \cdot H_{ij}(0)}. \tag{1}$$

Here, the summation is performed over every pair (i, j) of end-groups. The function $H_{ij}(t) = 1$ if end-groups i and j belong to the same cluster at time t, otherwise $H_{ij}(t) = 0$. The

autocorrelation times for these functions, given as their respective time integrals, are shown in fig. 3a). At the onset of micellization there is a large change in the temperature dependence of the autocorrelation times with much stronger dependence at lower T. This is consistent with the observed transition from spatial diffuse clusters containing relatively few end-groups at $T > T_x$ to more compact clusters containing many end-groups (micelles) at lower T (*i.e.*, $T < T_{\mathrm{m}}$).

In addition to microscopic structure and dynamics we investigated macroscopic viscoelastic properties of the self-associating system. We calculated the zero-shear rate viscosity (η) for the telechelic solutions using the Green-Kubo relationship [12] by integrating the stress tensor (σ_{xy}) autocorrelation function over time domain from zero to infinity. The viscosity for the self-associating system as well as the analogous system without end-group attraction [15] is shown in fig. 3a). As with cluster lifetimes and end-to-end vector decorrelation, the temperature dependence of the viscosity changes significantly at the onset of micellization, while for $T > T_x$ the viscosity is little influenced by the presence of attractive end-groups.

We also calculated the complex frequency (ω) dependent shear modulus ($G^*(\omega)$) given as [16]

$$G^*(\omega) = G'(\omega) + iG''(\omega) = i\omega \int_0^\infty e^{-i\omega t} G(t)\,\mathrm{d}t = i\omega \frac{V}{k_{\mathrm{B}}T} \int_0^\infty e^{-i\omega t} \langle \sigma_{xy}(t)\sigma_{xy}(0)\rangle\,\mathrm{d}t, \quad (2)$$

where $\langle \ldots \rangle$ denotes an equilibrium average of the stress-tensor autocorrelation function over phase space including circular permutations, V is the volume, and k_{B} is Boltzmann's constant. All values of the $G^*(\omega)$ have been normalized by the value of $G(\infty)$ for their respective temperature. The frequency-dependent mechanical susceptibility or loss modulus $G''(\omega)$ and storage modulus $G'(\omega)$ are shown in fig. 4a) and b), respectively. Beginning at high frequency, we observe a nearly temperature-independent process (A). This process also occurs above T_x and in systems without end-group attraction and can be associated with vibrational and librational motions of the chains. Process (B) is associated with translational motion of the end-groups within their clusters: the time scale of this process corresponds to the onset of caging (compare with fig. 2) and is only seen below T_x. Process (C), manifested only below T_x, is associated with the onset of end-groups hopping from their clusters, *i.e.*, the caging time, as can be seen by comparing the time scale of this process with end-group $\langle R^2 \rangle$ in fig. 2. Finally, process (D) corresponds to the onset of flow and is associated with polymer end-to-end relaxation and the break-up of end-group clusters. These latter correspondences are clearly seen when the dynamic susceptibility for the $V(t)$ and $C(t)$ (see eq. (1)), given as

$$\chi(\omega) = \omega\,\mathrm{Re}\left[\int_0^\infty \exp[-i\omega t]\Psi(t)\,\mathrm{d}t\right], \quad (3)$$

where $\Psi(t) = V(t)$ or $C(t)$, are compared with the mechanical susceptibility in fig. 4a). A lower-frequency shoulder, corresponding with the mechanical process (C) (*i.e.*, the onset of end-group hops), is also manifested in the dynamic susceptibility for the $V(t)$ and $C(t)$. At $T > T_x$, the features associated with end-group motion and cluster dynamics disappear in the viscoelastic response of the system, which then looks very much like the response of the analogous system without end-group attraction. Furthermore, comparison of the dynamic-mechanical response of the system below T_x with and without end-group attraction (see fig. 4) reveals that the transient elastic response of the solution is due entirely to end-group interactions, consistent with the assignments of mechanisms to the relaxation processes given above.

At temperatures below T_x where processes (C) and (D) are resolved, we have determined the relaxation time associated with these processes and plotted them in fig. 3a). As expected, the relaxation time for process (D) and its temperature dependence closely follows that of the

end-to-end vector relaxation and cluster lifetime. The higher-frequency process (C), associated with the onset of end-group hops, exhibits weaker temperature dependence following that of the caging time. The processes appear to merge around T_x. This behavior resembles the bifurcation of the primary low-frequency α process and secondary high-frequency sub-glass β process in glass-forming liquids and polymers [17]. For these materials it is commonly held that the β process reflects the fundamental underlying motion (*e.g.*, conformational transitions in polymers) whose cooperative manifestation leads to the primary relaxation. The parallel with the dynamic-mechanical relaxation observed in our self-associating solution is striking: below T_x we observe a relatively high-frequency process (C) reflecting the onset of fundamental motions ("hopping" of end-groups between clusters) that ultimately leads in a cooperative fashion to the destruction of clusters associated with the lower-frequency process (D). The higher apparent activation energy for the cooperative process results in a merging of their relaxation times at higher T. In fig. 3b) we show fits of the end-to-end vector relaxation time and η by the Vogel-Fulcher (VF) equation that is commonly used to describe the temperature dependence of the primary relaxation process in the glass transition region. The VF fit predicts a much smoother transition between low- and high-temperature regimes and especially deviate from the simulation data for $T \geq T_x$. The relatively sharp transition (in comparison with the VF prediction) between high- and low-T regimes for relaxation properties observed in our self-assembling polymer system may be the result of the reorganization of the diffuse clusters into more compact and longer-lived micelles below T_x. This kind of structural changes presumably does not occur in conventional glasses [18], so that it is not surprising that VF fits for our system are less than satisfactory. At any rate, it appears that our system more closely resembles a "strong" glass-forming material [19] with an Arrhenius-like temperature dependence of relaxation times. The inset of fig. 3b) shows the product of self-diffusion coefficients (D) and η as a function of $1/T$ which sharply increases upon cooling below T_x, a feature that is often observed in glass-forming liquids and attributed to fluid "dynamic heterogeneity" [20]. An onset of "dynamic heterogeneity" in glass-forming liquids for a crossover temperature about 1.2 times the calorimetric glass transition is another feature that seems to be similar to our simulations [21].

Finally, we note that the elastic plateau in the dynamic-mechanical response and the Arrhenius-like temperature dependence of the longest relaxation times for our system at $T < T_x$ resembles the behavior of entangled polymer solutions, an effect noted before by Groot and Agterof [7]. Furthermore, experiments on telechelic triblock copolymer solutions indicate a similar clustering transition to that observed in our simulations and relaxation processes and dynamic properties similar to both glass and network formation [22]. In our system at $T < T_x$ the temporal crosslinks responsible for the transient elastic response of the network are the end-group clusters, whose destruction results in the transition from elastic to liquid-like response. This phenomenological picture is further supported by the correspondence of the plateau shear modulus obtained from simulations with that yielded from simple network entropy elasticity analysis [23], where each telechelic polymer is assumed to be a stress-bearing chain segment. Similarities of dynamic features found for telechelic solutions with those observed in glass-forming liquids and entangled polymer solutions will be discussed in more detail in our forthcoming paper.

We have demonstrated that the onset of micellization results in a dramatic change in the temperature dependence of the important relaxation times in our model self-associating polymer system. Furthermore, micellization results in elastic dynamic-mechanical response over increasingly long time scales with decreasing temperature whose relaxation is dominated by the hopping of end-groups between clusters. At lower temperatures than those simulated here, the longest relaxation times of the system, associated with the destruction of the end-group

clusters, will become macroscopic and the system will undergo thermoreversible gelation, *i.e.*, it will exhibit elastic (solid-like) behavior on macroscopic time scales. The complex viscoelastic response of the material is due to the formation of a network of well-defined end-group clusters connected by the telechelic chains which influences dynamic and viscoelastic response only below the onset of micellization T_x, as evidenced by a) the presence of a geometrically percolating network of telechelic chains, which occurs at all temperatures investigated; b) the correspondence of the longest dynamic-mechanical relaxation time with the destruction of the clusters, as shown in figs. 3 and 4, c) the complete lack of elastic behavior without attractive end-groups, illustrated in fig. 4, and d) the close correspondence (within a factor of two) of the plateau shear modulus with that obtained from simple network entropy elasticity theory.

* * *

We would like to acknowledge the support of NASA Langley Research Center through grant NAG_12319.

REFERENCES

[1] Dudowicz J. *et al.*, *J. Chem. Phys.*, **111** (1999) 7116; **112** (2000) 1002; **113** (2000) 434; **114** (2001) 10573.
[2] Khalatur P. G. *et al.*, *Macromol. Theory Simul.*, **5** (1996) 713.
[3] Khalatur P. G. *et al.*, *J. Chem. Phys.*, **109** (1998) 9602.
[4] Khalatur P. G. *et al.*, *J. Chem. Phys.*, **110** (1999) 6039.
[5] Milchev A. *et al.*, *Macromolecules*, **34** (2001) 1881.
[6] Floriano M. A. *et al.*, *Langmuir*, **15** (1999) 3143.
[7] Groot R. D. and Agterof W. G. M., *Macromolecules*, **28** (1995) 6284.
[8] Kumar S. K. and Douglas J. F., *Phys. Rev. Lett.*, **87** (2001) 188301-1.
[9] Weeks J. D. *et al.*, *J. Chem. Phys.*, **54** (1971) 5237.
[10] Note that the simulations do not include explicit solvent molecules.
[11] `http://www.che.utah.edu/~gdsmith/mdcode/main.html`
[12] Allen M. P. and Tildesley D. T., *Computer Simulation of Liquids* (Oxford, New York) 1987.
[13] Shoemaker D. P. *et al.*, *Experiments in Physical Chemistry* (McGraw-Hill Book Co., New York) 1981.
[14] Donati C. *et al.*, *Phys. Rev. E*, **60** (1999) 3107.
[15] Simulations were performed at the same density and temperature as in case with sticky end-groups.
[16] Ferry J. D., *Viscoelastic Properties of Polymers* (Wiley, New York) 1980.
[17] Ediger M. D. *et al.*, *J. Phys. Chem.*, **100** (1998) 13200.
[18] Kob W., *J. Phys. Condens. Matter*, **11** (1999) R85.
[19] Angell C. A., *Proc. Natl. Acad. Sci. USA*, **92** (1995) 6675.
[20] Ediger M. D., *Annu. Rev. Phys. Chem.*, **51** (2000) 99.
[21] Rossler E., *Phys. Rev. Lett.*, **65** (1990) 1595.
[22] Raspaud E. *et al.*, *Macromolecules*, **27** (1994) 2956; **29** (1996) 1269.
[23] Flory P. J., *Principles of Polymer Chemistry* (Cornell University Press) 1953.